MRI-Based Assessment of Vertebral Deformity

E. A. Phillips[1], C. S. Rajapakse[1], M. J. Wald[1], Y. A. Bhagat[1], M. B. Leonard[2], F. W. Wehrli[1], and M. B. Leonard[2]
[1]Laboratory for Structural NMR Imaging, Department of Radiology, University of Pennsylvania, Philadelphia, PA, United States, [2]Childrens Hospital of Philadelphia, Philadelphia, PA, United States

Introduction: Vertebral fractures are among the most common outcomes of osteoporosis [1]. Early detection of vertebral deformities is important because patients with such deformities are known to be at elevated risk for further vertebral fractures [2]. The less than satisfactory performance of DXA-based BMD measurements [3] in predicting vertebral fracture susceptibility has spurred the search for other markers of bone quality. The purpose of this study was to evaluate the performance of a custom-built software tool for quantitative morphometry of spine on the basis of mid-line sagittal MR images. Towards this goal, we evaluated the intra-reader reproducibility of computing spinal deformity indices and their associations with age and gender as part of an ongoing translational study.

Methods: Image Acquisition: Forty-six healthy subjects (16 men, 30 women, 19-53 years of age) were studied by MRI following a previously described protocol [4]. In brief, multi-slice sagittal images of the midline spine were acquired on a 1.5-T (Siemens Sonata) scanner using the manufacturer's surface array coil and a turbo spin-echo sequence (TR/TE of 4000/13.6 ms, echo train length 8, bandwidth 31.25 kHz, NEX 2, field of view 40 × 30 cm, 0.78 × 0.78 mm^2 pixel size, and 5 mm slice thickness).
Vertebral Height and Width Measurements: Acquired spine images were taken as input to a custom-built semi-automatic software tool designed for quantitative spine morphometry. First, the midline sagittal slice was selected by scrolling through the imaging stack. Next, two anterior and two posterior landmarks (indicated by + in Figure 1) were manually placed at four "corners" of each visible vertebral body. Two additional landmarks were automatically generated and manually adjusted as needed at mid distance between anterior and posterior landmarks. Anterior height (H_a), posterior height (H_p), middle height (H_m), superior width (W_s), and inferior width (W_i) of each vertebral body were computed by taking the Euclidian distance between landmark points as illustrated in Figure 2. Spinal Deformity Quantification: Three types of deformities—wedge (W), biconcavity (B), and compression (C)--were calculated for each vertebral body by adapting an approach similar to that described by Eastell [4] shown in Figure 3, Equations (1-3). A continuous measure of total spinal deformity burden (referred as the spinal deformity index (SDI)) for vertebrae T9-L5 was computed as the weighted sum of W, B, and C deformities—to account for clinical relevance of each type of deformity—as previously described [3] with minor modifications (Equation 4). Evaluation of Intra-Operator Reproducibility: Images of four subjects were randomly selected for the purpose of testing the intra-operator reproducibility of the spinal deformity measurements. Measurements were performed on these four datasets as described above with one operator in quadruplicate at different times in a span of three days. Statistical Analysis: Differences in spinal deformity measurements among men and women were statistically evaluated using one-way ANOVA. Intra-operator reproducibility of each deformity type was evaluated by coefficients of variation (CV%).

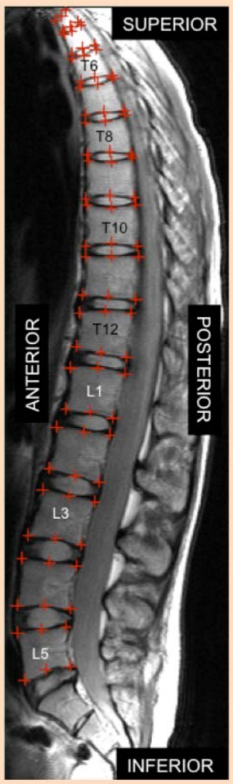

Figure 1. Mid-line sagittal MR image of the spine.

Results and Conclusions: Intra-reader reproducibility of vertebral deformity computations are summarized in Table 1 in terms of CV% for each type of deformity, which were well below the expected variations in vertebral deformity with age and disease. Correlations between vertebral deformities and age are shown in Table 2, revealing significant age dependence (except in wedge) in women even in the healthy and relatively young age (pre menopausal) group studied here. On the other hand, men did not show a correlation with age. The mean ages (men: 32.7; women: 35.78) were statistically non-significant. The mean SDI was higher in men (35.6) than women (33.8; $p = 0.007$, Figure 4) possibly due to men generally having higher vertebral width-height ratios than women [5,6], which result in higher compression deformity based on the current definition. Further investigations include: (a) developing a modified SDI formula that takes gender differences in vertebral anatomy, (b) determining the inter-dependence of each type of deformity in a given vertebral body, and (c) investigating the relationship between vertebral deformity indices with parameters of bone quality obtained at peripheral sites using recently developed structural and mechanical measures on the basis of high-resolution MRI techniques.

Patient	CV (%)		
	W	B	C
1	2.76	2.89	2.04
2	3.48	3.24	2.13
3	3.24	2.76	2.52
4	2.54	3.17	2.52

Table 1. Intra-reader reproducibility results.

Deformity	Female		Male	
	r	*p*	r	*p*
B	0.51	**0.004**	-0.17	NS
C	0.41	**0.024**	0.09	NS
W	-0.25	NS	-0.48	NS
SDI	0.42	**0.022**	-0.03	NS

Table 2. Deformity correlations with age of women and men.

References: [1] Cummings et al., Arch Intern Med, 1989. [2] Melton Osteoporosis Int, 1999. [3] Sarkar et al., J Bone Min Res, 2002:17. [4] Ladinsky et al., J Bone Min Res, 2008:23. [5] Eastell et al., J Bone Min Res, 1991:3. [6] Duan et al., J Bone Min Res, 2001:16. [7] Afari et al., Radiology, 2002:224.

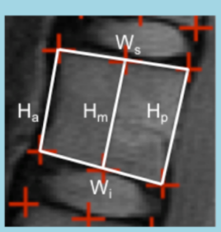

Figure 2. Enlargement of vertebral body and measurements.

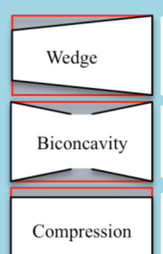

$$W = \frac{|H_p - H_a|}{\max(H_p, H_a)} \quad \text{Eq. (1)}$$

$$B = 1 - \frac{H_m}{\max(H_p, H_m, H_a)} \quad \text{Eq. (2)}$$

$$C = \frac{2H_p}{W_s + W_i} \quad \text{Eq. (3)}$$

Figure 3. Diagram of vertebral deformity and their calculations.

$$SDI_{T9L5} = \sum_{i=T9}^{L5} \left(B_i + 1.5W_i + 3C_i \right) \quad \text{Eq. (4)}$$

Figure 4. SDI comparison between men and women subjects.

p = 0.0067